Assignment of the Lowest Excited States of C_{70} and Evidence for Fluorescence from the S_2 State

A. Sassara, G. Zerza, and M. Chergui*

Institut de Physique Expérimentale, Université de Lausanne, CH-1015 Lausanne-Dorigny, Switzerland

Received: December 4, 1997; In Final Form: February 24, 1998

Highly structured fluorescence, phosphorescence, and fluorescence−excitation spectra of C_{70} in neon matrixes are reported. Fluorescence from both S_1 and S_2 states is observed, and these are identified as being of A_2' and E_1' symmetry and have gas-phase energies estimated at 15 560 and 15 725 cm^{-1}, respectively. A third singlet state is identified in the excitation spectrum and is proposed to be of A_2'' symmetry with an estimated gas-phase energy of 16 000 cm^{-1}. Finally, the phosphorescence is dominated by vibrational bands of e_1' symmetry pointing to the lowest triplet state of A_2' symmetry. Its energy lies at 12 588 cm^{-1} above that of the ground state in the neon matrix. From a comparison with data from the literature, the existence of a second triplet state of E_1' character is inferred, which lies about 165 cm^{-1} above the lowest triplet state, i.e., with the same energy separation as the lowest two singlet states.

1. Introduction

Most spectroscopic studies on fullerenes have concentrated on the C_{60} molecule in organic solvents or isolated in Shpol'skii matrixes.[1−3] From these spectroscopic data different assignments of the lowest singlet state were proposed. Using rare gas matrixes, especially neon or argon matrixes, we recently obtained highly structured fluorescence, phosphorescence, and fluorescence−excitation spectra, which allowed us to get a clear-cut assignment of the lowest-lying electronic states,[4−6] in good agreement with theoretical predictions.[6−9] For the other prominent fullerene, C_{70}, the situation is less clear.

According to INDO/CI calculations,[10] assuming D_{5h} symmetry for the C_{70} molecule, the lowest excited singlet state is of A_2' symmetry with an orbitally forbidden transition to the $^1A_1'$ ground state. It can, however, gain some intensity due to Herzberg−Teller (H−T) interaction induced by a_1'' and e_1' modes. Singlet states of E_1' and A_2'' symmetry with allowed electronic transitions to the ground state lie close to it. Both transitions $^1E_1' \leftrightarrow {}^1A_1'$ and $^1A_2'' \leftrightarrow {}^1A_1'$ should show a strong pure electronic origin in the spectra. In addition to this, H−T active modes of a_1', a_2', e_1'', and e_2' symmetry as well as Jahn−Teller (J−T) active modes of e_2' symmetry could show up in the spectra for the $^1E_1' \leftrightarrow {}^1A_1'$ transition, whereas only a_1' and e_1'' H−T modes could be present in case of the $^1A_2'' \leftrightarrow {}^1A_1'$ transition.

Fulara et al.[11] recorded the electronic absorption spectrum of C_{70} in neon matrixes and assigned the vibrational structure mainly to totally symmetric modes and their combinations. They concluded that the absorption in the 15500−17500 cm^{-1} range is due to only one electronic transition, namely, the allowed $^1E_1' \leftarrow {}^1A_1'$ transition. Despite this, some of the vibrational features in their spectra had to be left unassigned and mode frequencies well below 200 cm^{-1} had to be assumed, which, according to calculations,[9] are too low for this molecule.

Fluorescence spectra of C_{70} in various alkane Shpol'skii type matrixes at 1.5 K were reported.[12] They show strong site effects depending on sample preparation conditions. For specific preparation and excitation conditions, distinct sites could be selected and highly resolved fluorescence spectra were obtained. The authors assigned the vibrational structure in the spectra of C_{70} in *n*-pentane to different IR-active modes. This led them to the conclusion that fluorescence stems from the vibronically induced $^1A_2' \rightarrow {}^1A_1'$ transition.

Assuming that in the emission spectra of Warntjes et al.[12] and in the absorption spectra of Fulara et al.[11] the same states are involved (i.e., the lowest singlet state), discrepancies appear when comparing the frequencies of the first five most prominent modes in the fluorescence spectrum[12] with those in the absorption spectrum.[11] In the first case, we find a weak electronic origin, and bands at 420, 581, 677, 798, and 1089 cm^{-1} carry most of the intensity, whereas according to the assignment of ref 11, the absorption spectrum is dominated by a strong 0−0 transition followed by strong bands at 239, 272, 346, 356, and 615 cm^{-1}. For such a large molecule, frequency changes of this order between the ground state and the first excited state are unrealistic. The only way to solve this discrepancy would be to assume several electronic states in the observed range of the absorption spectrum.

Turning now to the triplet states, according to CNDO/S-CI calculations,[13] the three lowest triplet states are of A_2', E_1', and E_2' symmetry in order of increasing energy. In this work, the phosphorescence spectrum was simulated assuming the $^3A_2'$ to be the lowest triplet state. The transitions to the singlet ground state are induced by H−T and by spin−orbit interaction as well. The possible modes in the phosphorescence spectra for the $^3A_2' \rightarrow {}^1A_1'$ transition are a_1'', a_2'', e_2'', and e_1'. Those with the largest activity are determined to be of e_1' symmetry.[13]

Phosphorescence spectra of C_{70} in organic solvents and Shpol'skii matrixes have been reported by different groups.[11,14,15] Argentine et al.[15] identified the $^3E_1'$ state as the lowest triplet state using ac Stark modulated phosphorescence measurements. Lifetimes of the order of 50 ms have been determined for the lowest triplet state of C_{70} in "glassy" solutions.[16] Just as for the fluorescence, Warntjes et al.[12] observed multiplet structures in the vibronic bands of the phosphorescence that are due to different sites. A strong dependence of the electronic origin intensity on the solvent was attributed to a matrix-induced static lowering of the symmetry. From the symmetry of the inducing modes, a mixed A_2'/E_1' character was proposed for the lowest triplet state.

In this work fluorescence and fluorescence−excitation spectra of C_{70} in solid neon will be presented. By comparision of both

S1089-5639(98)00422-8 CCC: $15.00

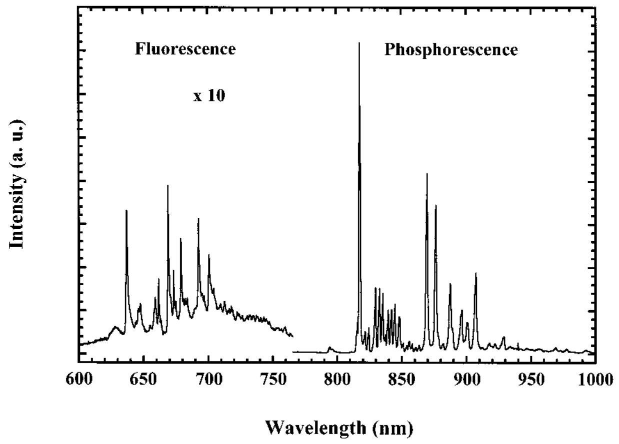

Figure 1. Emission spectrum of C_{70} in solid neon for excitation at 470 nm. Resolution is ~5 cm^{-1}.

types of spectra, an assignment of the lowest three singlet states is proposed. In addition, we deal with the phosphorescence spectra of C_{70} in neon matrixes. Starting from the weak electronic origin, the main inducing bands are assigned to modes of e_1' symmetry. From this, the $^3A_2'$ state is deduced to be the lowest triplet state.

2. Experimental Section

The samples were prepared by flowing neon gas (99.998% purity) through a vapor of C_{70} (Hoechst, "Gold Grade", 99.4% purity) produced in a stainless steel oven by heating the C_{70} soot to about 500 °C. The gas mixture was deposited on an MgF_2 sample holder cooled to 4 K by a liquid helium flow cryostat. Under comparable preparation conditions and using an interferomertric method, we determined in ref 4 the concentration of C_{60} in solid Ne to be of the order of 0.1%. Considering that the vapor pressure of C_{70} is lower, this value should be an upper limit for the concentration of C_{70} in solid Ne. The samples were irradiated by laser light from an optical parametric oscillator pumped by the third harmonic wave of an injection-seeded Nd:YAG laser. The laser system is tunable from 450 to 690 nm for the signal wave with a line width of 0.2 cm^{-1}. Fluorescence and phosphorescence spectra were recorded using a 0.39 m monochromator equipped with a liquid-nitrogen-cooled CCD camera with a spectral resolution of 5 cm^{-1} for a 1200 lines/mm grating and 50 μm slits. For the high-resolution fluorescence spectra, a 0.67 m McPherson monochromator was also used, reaching a resolution of 2 cm^{-1} for an 1800 lines/mm grating and 50 μm slits. For recording excitation spectra, the emitted light was detected by a photomultiplier (Hamamatsu R636−10, sensitivity range: 185 nm to 930 nm) and recorded using either a Boxcar integrator for the fluorescence or a photon-counting system for the phosphorescence. All fluorescence and phosphorescence spectra shown here are corrected for the spectral response of the CCD detector and the efficiency of the gratings.

3. Results and Discussion

Figure 1 shows the emission spectrum of C_{70} in Ne matrixes for excitation at 470 nm. Contrary to C_{60} isolated in solid neon where only fluorescence was observed,[4,6] C_{70} phosphorescence is also present along with the fluorescence. Two groups of bands can be distinguished in Figure 1, one centered around 670 nm and the other around 870 nm. On the basis of previous work,[12,14,15] the former is recognized as the fluorescence while the latter as the phosphorescence. Compared with the maximum peak in fluorescence, the maximum peak intensity in phosphorescence is about 20 times stronger (Figure 1). A more detailed analysis of the fluorescence and phosphorescence is presented below.

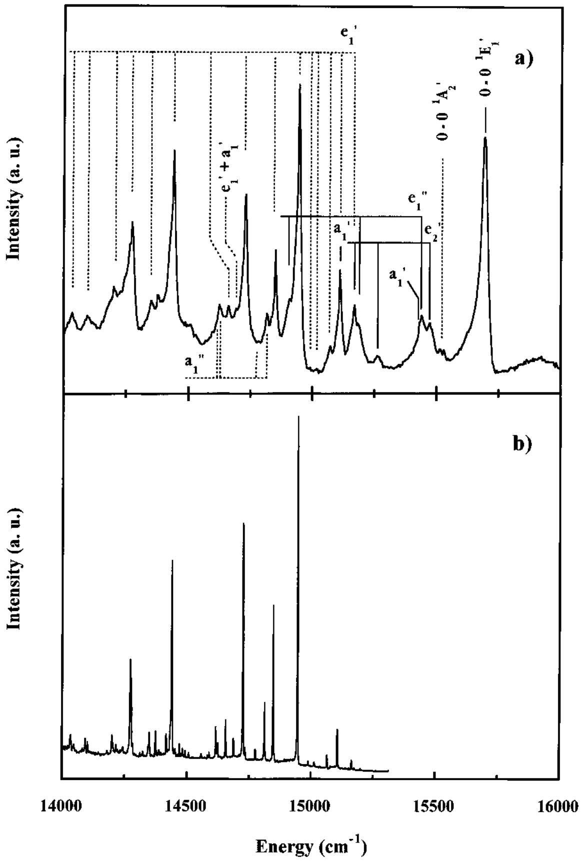

Figure 2. Fluorescence spectrum of C_{70} in solid neon for (a) λ_{exc} = 470 nm (21 277 cm^{-1}) and (b) λ_{exc}= 644.16 nm (15 524 cm^{-1}), which corresponds to the electronic origin of the $^1A_2'$ state. In this case the line width is reduced to 2 cm^{-1} (i.e., limited by our resolution). Solid marks refer to the $^1A_2' \rightarrow {}^1A_1'$ transition and dotted marks to the $^1E_1' \rightarrow {}^1A_1'$ transition. The details of the assignments are given in Table 1.

3.1. Fluorescence Spectrum of C_{70}. Figure 2a shows a fluorescence spectrum of C_{70} in solid neon in the region of 14000−16000 cm^{-1}. The vibrational structure is quite similar to the fluorescence spectra in *n*-heptane or *n*-pentane.[12] Assuming that the strongest peak at 14 945 cm^{-1} in our spectrum (Figure 2) corresponds to the most prominent band at 14 637 cm^{-1} in the work of Warntjes et al.[12] (the shift between the two is due to solvent effects), we can find a near one-to-one correspondence between the two spectra. In this case, the electronic origin in the neon spectrum should be the weak shoulder at 15 524 cm^{-1} (Figure 2), since the 14 945 cm^{-1} peak lies some 580 cm^{-1} red of the origin according to ref 12. This is confirmed by exciting directly at the electronic origin (644.16 nm, 15 524 cm^{-1}), which yields the fluorescence spectrum in Figure 2b. We find the seven most prominent bands at frequencies 412, 579, 671, 707, 793, 1082, and 1250 cm^{-1} from the origin (dotted tick marks in Figure 2), which all correspond to bands observed by Warntjes et al.[12]

The following points should be noted. (a) There are two emission systems, one with the origin at 15 524 cm^{-1} (dotted marks in Figure 2a) and a second one with an origin at 15 691 cm^{-1} (solid line in Figure 2a). Indeed, a group of peaks (solid tick marks in Figure 2a) disappears upon excitation at the 15 524 cm^{-1} band (Figure 2b). (b) The line width of the peaks narrows down by nearly 1 order of magnitude, from about 15 cm^{-1} in Figure 2a to about 2 cm^{-1} in Figure 2b upon excitation at 644.16

TABLE 1: Assignments of the Fluorescence Spectrum of C_{70} in Solid Neon[a]

energy (cm^{-1})	shift (cm^{-1})	assignt	shift (cm^{-1})	assignt
15 691			0	origin of $^1E_1' \rightarrow {}^1A_1'$
15 524	0	origin of $^1A_2' \rightarrow {}^1A_1'$		
15 470			221	e_2' (224)
15 440			251	e_1'' (252)
15 428			263	a_1' (260)
15 265			426	e_2' (436)
15 181			510	e_1'' (508)
15 166	358	e_1' (365 c)	525	e_2' (521)
15 112	412	e_1' (418)	579	a_1' (572)
15 068	456	e_1' (458)		
15 014	510	e_1' (510)		
14 991	533	e_1' (535)		
14 945	579	e_1' (578)		
14 907			784	e_1'' (771)
14 853	671	e_1' (674)		
14 813	707	a_1'' (721 c)		
14 777	747	a_1'' (784 c)		
14 731	793	e_1' (795)		
14 693	831	$e_1' + a_1'$ (838)		
14 663	861	e_1' (884 c)		
14 626	898	a_1'' (901 c)		
14 616	908	a_1'' (901 c)		
14 442	1082	e_1' (1086)		
14 350	1174	e_1' (1224 c)		
14 274	1250	e_1' (1252)		
14 206	1318	e_1' (1321)		
14 099	1425	e_1' (1430)		
14 038	1486	e_1' (1460)		

[a] The numbers given in parentheses correspond to experimental results from IR[19,20] and Raman studies[17,18] and from QCFF/PI calculations (marked with c) from ref 9 for the ground-state vibrational frequencies of C_{70} (in cm^{-1}).

nm (15 524 cm^{-1}). This shows the importance of inhomogeneous broadening. Whereas at high excitation energy a distribution of matrix sites is populated (Figure 2a), excitation directly at the lowest electronic origin selects molecules in a restricted group of sites (Figure 2b).

In Table 1, we compare our measured mode frequencies with the results of QCFF/PI calculation[9] and experimental values from Raman[17,18] and IR[19,20] studies and propose an assignment. For the band system in Figure 2b and the corresponding bands in Figure 2a, all of the spectral features are found to have e_1' symmetry except three of a_1'' symmetry. There remains the strong band at 15 691 cm^{-1} and some weaker broad features between 14 800 and 15 500 cm^{-1} (solid tick marks in Figure 2a), which do not correspond to any band in the spectra of Warntjes et al.[12] The only possibility is to assign them to emission from a higher-lying electronic state. In fact, the band assigned as the electronic origin in the absorption spectrum in solid neon[11] lies within 1 cm^{-1} at the same position as the 15 691 cm^{-1} band in the fluorescence spectrum of Figure 2a. This is confirmed by the fluorescence−excitation spectrum (Figure 3), which is discussed in the next section. Taking this band as a second electronic origin 167 cm^{-1} higher in energy than the first one, the unassigned features in the fluorescence spectrum show up at 221, 251, 263, 426, and 510 cm^{-1} from it. These are attributed to the totally symmetric and nontotally symmetric modes, a_1', e_2', and e_1'', on the basis of frequencies (see Table 1).[9]

Most of the intensity in the fluorescence spectrum is due to the lowest electronic state with a weak origin at 15 524 cm^{-1} (Figure 2). The transition to the ground state is orbitally forbidden and induced by Herzberg−Teller coupling. The observed modes are of e_1' and a_1'' symmetry (Table 1). The only electronic transition in this energy range giving rise to these kinds of modes is the $^1A_2' \rightarrow {}^1A_1'$ transition, in agreement with the assignment of ref 12.

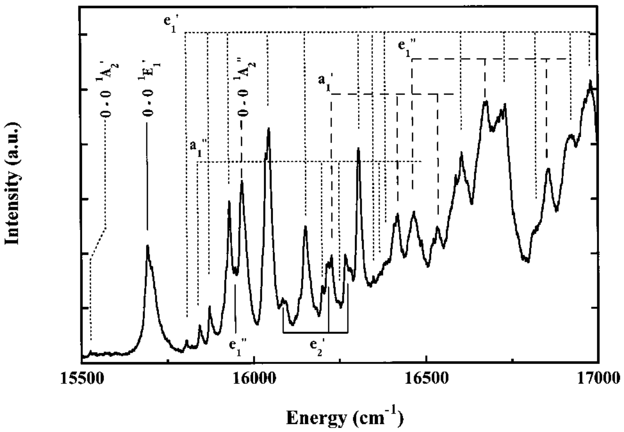

Figure 3. Fluorescence−excitation spectrum of C_{70} in solid neon for the 14 442 cm^{-1} (692.4 nm) emission. Solid marks, dotted marks, and dashed marks refer to the $^1A_2' \leftarrow {}^1A_1'$, $^1E_1' \leftarrow {}^1A_1'$, and $^1A_2'' \leftarrow {}^1A_1'$ transitions. The details of the assignments are given in Table 2.

For the second, strong electronic origin at 15 691 cm^{-1} (Figure 2a), both totally symmetric a_1' and H−T active e_2' and e_1'' modes show up (Table 1). Such modes can only be due to the allowed $^1E_1' \rightarrow {}^1A_1'$ transition. All vibronic bands, which correspond to this higher electronic state, vanish under selective excitation of the lower electronic state (Figure 2b). As expected for an orbitally allowed transition in large molecules in the limit of small geometry changes under one-electron excitation, the intensity drops off from the strong pure electronic origin band to the higher vibronic bands (solid lines in Figure 2a).

Different from the case of C_{60} in solid neon,[4,6] C_{70} fluorescence stems both from S_1 and S_2 electronic states, which are separated by an energy gap of 167 cm^{-1}. The energy spacing between these two lowest electronic states is smaller than the smallest vibrational quantum of the molecule (~200 cm^{-1}) so that energy cannot be converted to vibrational energy of the molecule. The lifetime of S_2 fluorescence could not be measured, since it is shorter than the laser pulse width of 5 ns.

3.2. Fluorescence−Excitation Spectrum of C_{70}. The emission band at 14 442 cm^{-1} in the fluorescence spectrum (Figure 2) was chosen for recording the excitation spectrum, which is shown in Figure 3. This band is attributed to the 1082 cm^{-1} e_1' mode (Table 1) of the fluorescence from the lowest singlet state of A_2' symmetry. There is a strong correspondence of the excitation spectrum in neon matrixes (Figure 3) with the resonant two-photon ionization spectrum of C_{70} in molecular beams reported by Haufler et al.,[21] in particular in the 15750−16400 cm^{-1} region. A comparison of the most prominent peaks in this region for both spectra indicates that the absorption bands are shifted by ~35 cm^{-1} to lower energies in the neon matrixes. This is identical with the matrix shift found for C_{60} in neon matrixes.[4] Our excitation spectrum shows a one-to-one correspondence with the absorption spectrum reported by Fulara et al.[11] In their work, most of the observed vibrational structures were assigned to totally symmetric modes starting from only one electronic origin, namely, the$^1E_1'$ state. In the following, we will show that the $^1E_1'$ state is only responsible for a minor part of the vibronic structures in the absorption (excitation) spectrum.

The electronic origin at 15 691 cm^{-1} is common to the excitation spectrum (Figure 3) and the fluorescence spectrum (Figure 2a). About this origin, only four weak bands with e_2' and e_1'' symmetry are found to be common to both types of

TABLE 2: Assignments of the Fluorescence−Excitation Spectrum of C_{70} in Solid Neon[a]

energy (cm^{-1})	shift (cm^{-1})	assign	shift (cm^{-1})	assign	shift (cm^{-1})	assign
15 524	0	origin of $^1A_2' \leftarrow {}^1A_1'$				
15 691			0	origin of $^1E^{1\prime} \leftarrow {}^1A_1'$		
15 805	281	e_1' (330)				
15 844	320	a_1'' (341 c)				
15 874	350	e_1' (365 c)				
15 928	404	e_1' (418)				
15 966					0	origin of $^1A_2'' \leftarrow {}^1A_1'$
15 943			252	e_1'' (252)		
16 047	523	e_1' (578)				
16 088			397	e_2' (436)		
16 149	625	e_1' (674)				
16 202	678	a_1'' (720 c)				
16 217			526	e_2' (521)		
16 224					258	a_1' (260)
16 247	723	a_1'' (784 c)				
16 271			580	a_1' (572)		
16 309	785	e_1' (793)				
16 349	825	e_1' (884 c)				
16 367	843	a_1'' (901 c)				
16 384	860	e_1' (938 c)				
16 415					449	a_1' (457)
16 461					495	e_1'' (508)
16 537					571	a_1' (572)
16 605	1081	e_1' (1086)				
16 674					708	e_1'' (715)
16 728	1204	e_1' (1252)				
16 820	1296	e_1' (1321)				
16 850					884	e_1'' (916 c)
16 918	1394	e_1' (1430)				
16 979	1455	e_1' (1460)				

[a] The numbers given in parentheses correspond to results from IR[19,20] and Raman studies[17,18] and from QCFF/PI calculations (marked with c)[9] for the ground-state vibrational frequencies of C_{70} (in cm^{-1}).

spectra (solid tick marks in Figures 2 and 3), whereas for all the strong peaks, no mirror image can be found about this origin. This means that the main part of the excitation (or absorption) spectrum cannot be due to the $^1E_1'$ state. Some of the weak bands in Figure 2 are not found in the excitation spectrum (Figure 3), since they are shaded by stronger bands due to other states.

Looking more carefully at 15 524 cm^{-1} in Figure 3, where the origin of the A_2' state is proposed for the fluorescence, a weak band can be seen. Following the assignment of the fluorescence spectrum, we assign this band to the electronic origin for the absorption spectrum of the $^1A_2'$ state. This is confirmed by a comparison of the excitation and the fluorescence spectra (Figures 2 and 3). There is a strong correspondence for most of the bands on both sides of this origin. Two bands (the first e_1' and a_1'' in Figure 3) appear in the excitation spectrum, which are not observed in the fluorescence spectrum, since they are hidden by stronger peaks (Figure 2a). On the other hand, some weak bands of the fluorescence spectrum are not observed in the excitation spectrum, since they overlap with stronger lines from the other electronic states. Starting from the two origins $^1E_1'$ and $^1A_2'$, the vibrational band frequencies are determined and listed in Table 2 together with the proposed assignments corresponding to the different electronic origins. The frequencies of the vibrational modes match well the calculated[9] and measured ground-state frequencies[17−20] of C_{70}, taking into account a small decrease of less than 5%. Only the e_2' mode of the $^1E_1' \leftarrow {}^1A_1'$ transition with 397 cm^{-1} and the e_1' mode of the $^1A_2' \leftarrow {}^1A_1'$ transition with 523 cm^{-1} (Table 2) suffer a decrease of the order of 10% relative to their measured ground-state frequencies (Table 1).

There are still a number of bands that are left unassigned in the excitation spectrum and have no counterparts in the fluorescence spectrum (dashed tic marks in Figure 3). Let us now concentrate on the band at 15 966 cm^{-1}. If we assume it to be the origin of a third electronic state, then it should be due to an allowed transition with the ground state because of its relatively strong intensity (compare with the other allowed transition band at 15 691 cm^{-1}). Starting from this origin, all the peaks marked with dashed tic marks in Figure 3 can be associated with modes of a_1' and e_1'' symmetry (Table 2). From calculations,[10] the only state in this energy range with an allowed transition to the ground state is of A_2'' symmetry and the observed mode symmetries are the ones expected in this case.

However, most of the vibronic features in the excitation and absorption spectrum up to 17 000 cm^{-1} originate from the A_2' and A_2'' electronic states. Above this energy the excitation spectrum becomes congested and a clear-cut assignment is no longer possible without the help of CNDO/S calculations as, for instance, was done in the case of C_{60}.[6]

The presence of the $^1E_1'$ state in the excitation spectrum of an $^1A_2'$ emission band clearly shows that energy funnels down to the latter state via $^1E_1'$ despite the gap of 167 cm^{-1} between them. As mentioned above, this energy cannot be converted to internal modes of the molecule. On the other hand, it is likely that the $^1E_1' \rightarrow {}^1A_2'$ relaxation takes place by a reversible intersystem crossing such as $^1E_1' \rightarrow T_n \rightarrow {}^1A_2'$, where T_n represents the vibronic manifold of near-lying triplet states. This is confirmed by the excitation spectrum of the phosphorescence bands, which is identical to that of the fluorescence (Figure 3).

Williams and Verhoeven[22] determined the fluorescence quantum yield of C_{70} in various organic solvents to be of the order of 5×10^{-4} in various solvents. The lifetime is found to be 600−700 ps in most reports.[22−24] All of these reports concern C_{70} in hydrocarbon solvents or matrixes, and it is not clear whether both S_1 and S_2 states are observed. Still, the low values for the quantum yield of fluorescence points to a very inefficient population mechanism from higher-lying states (triplets or singlets), or to a highly efficient quenching channel that can only be to the triplet states, or to a combination of

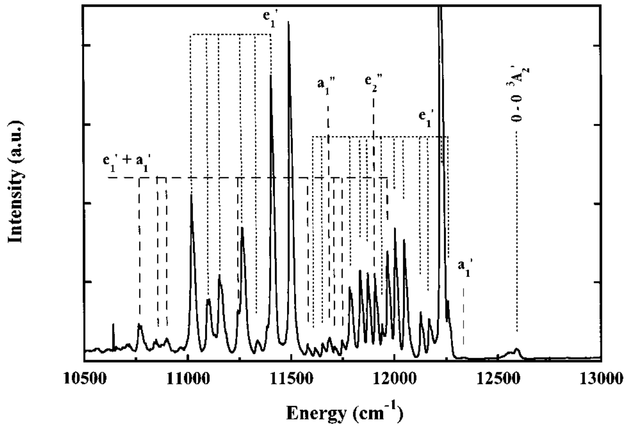

Figure 4. Phosphorescence spectrum of C_{70} in solid neon, excited at 470 nm (21 277 cm^{-1}). The details of the assignments are given in Table 3. Resolution is ~5 cm^{-1}.

both. The resemblance between the excitation spectra of the fluorescence and the phosphorescence suggests that the route leading to phosphorescence is common to the singlet states that yield the fluorescence.

The occurrence of S_2 emission for a molecular object as large as C_{70} is quite remarkable, especially in view of the fact that the molecule is in a "solvent" (solid Ne). The few cases where S_2 emission has been observed in polyatomic molecules concern the azulenes,[25,26] the pyrenes,[27,28] and naphthalene.[29] C_{70}, on the other hand, is the largest molecule so far found to produce an S_2 fluorescence. Its presence reflects the fact that bottlenecks to intramolecular nonradiative relaxation can occur despite the high density of states. Work is in progress to analyze the origin of such a bottleneck to electronic relaxation.

In summary, three excited electronic states have been identified, which account for the vibrational structure in the fluorescence−excitation spectrum up to 17 000 cm^{-1}. The lowest two, $^1A_2'$ at 15 524 cm^{-1} and $^1E_1'$ at 15 691 cm^{-1}, have counterparts in the fluorescence spectrum. A third electronic state of A_2'' symmetry lying 442 cm^{-1} above the lowest one has been identified, which accounts for additional vibronic structure in the fluorescence−excitation spectrum. From the gas-to-matrix shift of 35 cm^{-1} (see above), the gas-phase energies of the $^1A_2'$, $^1E_1'$, and $^1A_2''$ states are estimated to be 15 559, 15 626, and 16 001 cm^{-1}, respectively.

3.3. Phosphorescence Spectrum of C_{70}. Figure 4 shows the phosphorescence spectrum in the spectral range between 10 500 and 13 000 cm^{-1}. The intensity scale is chosen in such a way as to be able to show also the weak features in the spectrum. A lifetime of 52 ± 2 ms has been measured for all of the phosphorescence bands. The small peak at 12 588 cm^{-1} can clearly be assigned to the electronic origin. The origin of the weak shoulder on the left is unclear. It could be due to a second matrix site, but a similar shoulder does not appear for the vibronic bands that stem from this state and that show up at lower frequencies in Figure 4. The intensity distribution of the phosphorescence bands resembles strongly that of C_{70} in *n*-heptane and *n*-pentane reported by Warntjes et al[12] except for the relative intensity of the origin band to the other vibronic bands. Whereas these authors observe a relatively strong electronic origin ($^1/_7$ of the strongest vibronic band), in our case the intensity of the origin band is about 50 times smaller than the strongest vibronic band. A strong solvent dependence of the origin was also reported by Argentine et al.[15] with heavier solvents enhancing the origin significantly compared with the rest of the phosphorescence bands. The occurrence of phosphorescence bands for C_{70} results from spin−orbit coupling, while vibronic coupling can in addition induce vibrational modes. The vibronic perturbation is a predominantly intramolecular effect[13] and should not be too much affected by the environment. On the other hand, the spin−orbit perturbation is an electronic effect that is enhanced by the presence of perturbers with high polarizabilities, which tend to mix the states of singlet and triplet character. Thus, an enhanced spin−orbit coupling due to the presence of heavy perturbers will enhance the whole progression and not just the origin (or other members) with respect to the rest of the progression. In this respect and even though all the bands in Figure 4 originate from the same state, the solvent-dependent intensity variation of the origin relative to the other bands cannot be interpreted in terms of enhanced spin−orbit coupling despite the fact that of all the environments in which C_{70} phosphorescence has been observed,[12,15] neon has the lowest polarizability. On the other hand, reducing the molecular symmetry by solvent caging effects could significantly alter the relative intensity of the origin and the other members of a progression. Our preliminary results in argon matrixes show a strong increase of the pure electronic origin compared with results in neon matrixes. It may be argued that the more rigid the matrixes, the more efficient is the reduction of molecular symmetry. Of all the media where phophorescence has been reported, neon is the softest. If this were the case, then the origin should be even weaker in liquid media.

With our choice of the electronic origin, the first strong band in Figure 4 lies at an energy of 361 cm^{-1} from the origin. Negri and Orlandi[9] calculated the $e_1'(2)$ mode at nearly this frequency. If we compare the other prominent peaks in the spectrum with the results of their calculations, we find good agreement between the two sets of data (see Table 3). We have thus identified 19 of the 21 possible modes of e_1' symmetry predicted by Negri and Orlandi[9] (see Table 3). In addition to these, smaller contributions from the lowest totally symmetric a_1' mode at 255 cm^{-1} and from modes of a_1'', a_2'', and e_2'' symmetries are also present. In Table 3, we propose an assignment and compare our mode frequencies (from Figure 3) with experimental results from IR and Raman studies[17−20] and with results from calculations.[9] Coming back to symmetry considerations concerning transitions from the lowest triplet states to the ground state, the sole state involving mainly e_1' modes is the $^3A_2' \rightarrow {}^1A_1'$.[9] This assignment was already proposed by Negri and Orlandi[13] in their discussion of Argentine et al.'s phosphorescence spectrum.[15] Given the wealth in spectral features of Figure 4, a close comparison can be made with the calculated oscillator strength of ref 13. Unfortunately, the comparison shows poor agreement between experimental and calculated intensities.

Finally, Argentine et al.[15] found an additional band for C_{70} in MCH glass matrixes that does not show up in our phosphorescence spectrum. This band lies some 165 cm^{-1} above the electronic origin of the $^3A_2'$ state, and it disappears for temperatures below ~30 K. Although the lifetime of the rest of the phosphorescence bands was measured to be ~100 ms at 77 K, the lifetime of the additional band was too short to be measured by their apparatus and was <2 μs. Argentine et al. concluded that this additional band is caused by emission from a higher electronic state, which is thermally activated. This state must have triplet character, since it lies ~165 cm^{-1} above T_1, whereas the T_1-S_1 splitting inferred from the present study is ~2940 cm^{-1} (see Tables 2 and 3). Thus, the T_1-T_2 splitting is ~165 cm^{-1}, and it is remarkable to note that it is identical with the S_1-S_2 splitting. According to theory, the next-higher

TABLE 3: Assignments of the Phosphorescence Spectrum of C_{70} in Solid Neon[a]

energy (cm^{-1})	shift (cm^{-1})	assignt
15 588	0	origin of $^3A_2' \rightarrow {}^1A_1'$
12 333	255	a_1' (260)
12 258	330	e_1' (330 c)
12 227	361	e_1' (365 c)
12 167	421	e_1' (418)
12 129	459	e_1' (458)
12 046	542	e_1' (535)
12 005	583	e_1' (578)
11 969	619	$e_1' + a_1'$ (616)
11 939	649	e_1' (652 c)
11 908	681	e_2'' (687 c)
11 871	717	e_1' (714 c)
11 840	748	e_1' (759 c)
11 788	800	e_1' (795)
11 753	835	$e_1' + a_1'$ (838)
11 716	872	$e_1' + 2a_1'$ (871)
11 686	902	a_1'' (901 c)
11 655	933	e_1' (938 c)
11 619	969	e_1' (969 c)
11 582	1006	$e_1' + a_1'$ (1003)
11 500	1088	e_1' (1086)
11 412	1176	e_1' (1224 c)
11 340	1248	e_1' (1252)
11 268	1320	e_1' (1321)
11 247	1341	$e_1' + a_1'$ (1343)
11 159	1429	e_1' (1430)
11 103	1485	e_1' (1460)
11 026	1562	e_1' (1560)
10 897	1691	$e_1' + a_1'$ (1684)
10 845	1743	$e_1' + a_1'$ (1749)
10 768	1820	$e_1' + a_1'$ (1817)

[a] The numbers given in parentheses correspond to experimental results from IR[19,20] and Raman studies[17,18] and from QCFF/PI calculations (marked with c)[9] for the ground-state vibrational frequencies of C_{70} (in cm^{-1}).

triplet state has E_1' symmetry and it should therefore have the same vibronically induced bands as the singlet state of same symmetry. Since the latter is characterized by an intensity falloff of the vibronically induced false origin bands, it is no wonder that the additional band appears isolated in the spectrum of Argentine et al.,[15] since all the false origins will be shaded by the bands belonging to T_1. The presence of T_2 emission for C_{70} has a different origin than that of S_2 emission. T_2 emission occurs because of thermal equilibration between T_1 and T_2. T_1 being a long-lived state, for low temperatures only the latter is populated as is the case in our spectra (Figure 3). On the other hand, S_2 occurs because of a competition between the radiative transition $S_2 \rightarrow S_0$, which has an allowed character in C_{70}, and the nonradiative channels that depopulate S_2. In that respect it represents a deviation to Kasha's rule, which states that in aromatic molecules, emission occurs from the lowest electronic state of a given multiplicity.

4. Conclusions

By use of fluorescence and fluorescence−excitation spectroscopy of C_{70} in neon matrixes, the three lowest singlet states have been identified. Fluorescence stemming from two singlet states $^1A_2'$ at 15 524 cm^{-1} and $^1E_1'$ at 15 691 cm^{-1} has been observed. A third singlet state was identified in the excitation spectrum. It is found to be of $^1A_2''$ symmetry and to have an energy of 15 966 cm^{-1} above the ground state. In addition, the fluorescence from the lower electronic state $^1A_2'$ could be obtained separately by exciting directly at its electronic origin, thus showing the importance of inhomogeneous contributions in the matrix spectra of C_{70}. The observed phosphorescence has a lifetime of 52 ms from the lowest triplet state. Most of the 21 possible e_1' modes, which should show the strongest activity in the phosphorescence spectra, are found. The phosphorescence is due to the $^3A_2' \rightarrow {}^1A_1'$ transition with an origin at 12 588 cm^{-1}. For all these states, gas-phase energies can be inferred by adding the gas-to-matrix shift of ∼35 cm^{-1} inferred from a comparison of our excitation spectra (Figure 3) with the gas-phase two-photon ionization data of ref 21.

Complementing our observations with those of Argentine et al.,[15] we can predict the existence of an additional triplet state of E_1' symmetry, which lies some 165 cm^{-1} above the $^3A_2'$ state.

C_{70} is the largest molecule for which such an S_2 emission has so far been reported. The analysis of intramolecular relaxation mechanisms leading to it is now underway.

Acknowledgment. We are grateful to La Fondation Herbette de l'Université de Lausanne for its financial support in the acquisition of the McPherson monochromator.

References and Notes

(1) Leach, S.; Vervloet, M.; Desprès, A.; Bréheret, E.; Hare, J. P.; Dennis, T. J.; Kroto, H. W.; Taylor, R.; Walton, D. R. M. *Chem. Phys.* **1992,** *160*, 451.

(2) van den Heuvel, D. J.; van den Berg, G. J. B.; Groenen, E. J. J.; Schmidt, J.; Holleman, I.; Meijer, G. *J. Phys. Chem.* **1995**, *99*, 11644.

(3) van den Heuvel, D. J.; Chan, I. Y.; Groenen, E. J. J.; Matsushita, M.; Schmidt, J.; Meijer, G. *Chem. Phys. Lett*. **1995**, *223*, 284.

(4) Sassara, A.; Zerza, G.; Chergui, M. *J. Phys.* **1996**, *B29*, 4997.

(5) Sassara, A.; Zerza, G.; Chergui, M. *Chem. Phys. Lett*. **1996**, *261*, 213.

(6) Sassara, A.; Zerza, G.; Chergui, M.; Negri, F.; Orlandi, G. *J. Chem. Phys*. **1997**, *107*, 8731.

(7) Negri, F.; Orlandi, G.; Zerbetto, F. *J. Phys. Chem*. **1996**, *100*, 10849.

(8) Negri, F.; Orlandi, G.; Zerbetto, F. *J. Chem. Phys*. **1992**, *97*, 6496.

(9) Negri, F.; Orlandi, G. J. Phys. *B29*, 5049 1996

(10) Feng, J.; Li, J.; Li, Z.; Zener, M. C. *Int. J. Quantum Chem.* **1991**, *39*, 331.

(11) Fulara, J.; Jakobi, M.; Maier, J. P. *Chem. Phys. Lett*. **1993**, *206*, 203.

(12) Warntjes, J. B. M.; Holleman, I.; Meijer, G.; Groenen, E. J. J. *Chem. Phys. Lett*. **1996**, *261*, 495.

(13) Negri, F.; Orlandi, G. *J. Phys.* **1996**, *B29*, 5077.

(14) Argentine, S. M.; Francis, A. H.; Chen, C.-C.; Lieber, C. M.; Siegel, J. S. *J. Phys. Chem.* **1994**, *98*, 7350.

(15) Argentine, S. M.; Klotz, K. T.; Francis, A. H. *J. Am. Chem. Soc*. **1995**, *117*, 11762.

(16) Wasielewski, M. R.; O'Neil, P. M.; Lykke, K. R.; Pellin, M. J.; Gruen, D. M. *J. Am. Chem. Soc*. **1991**, *113*, 2774.

(17) Meilunas, R.; Chang, R. P. H.; Liu, S.; Jensen, M.; Kappes, M. M. *J. Phys. C* **1991**, *70*, 5128.

(18) Jishi, R. A.; Dresselhaus, M. S.; Wang, K.-A.; Zhou, P.; Rao, A. M.; Eklund, P. C. *Chem. Phys. Lett.* **1993**, *206*, 187.

(19) Bethune, D. S. Meijer, G.; Tang, W. C.; Rosen, H. J.; Golden, W. G.; Seki, H.; Brown, C. A.; De Vries, M. S. *Chem. Phys. Lett*. **1991**, *179*, 181.

(20) Bowmar, P.; Hayes, W.; Kurmoo, M.; Pattenden, P. A.; Green, M. A.; Day, P.; Kikuchi, K. *J. Phys.* **1994**, *C6*, 3161.

(21) Haufler, R. E.; Chai, Y.; Chibante, L. P. F.; Fraelich, M. R.; Weisman, R. B.; Curl, R. F.; Smalley, R. E. *J. Chem. Phys*. **1991**, *95*, 2197.

(22) Williams, R. M.; Verhoeven, J. W. *Chem. Phys. Lett*. **1992**, *194*, 446.

(23) Kim, D.; Lee, M.; Suh, Y. D.; Kim, S. K. *J. Am. Chem. Soc.* **1992**, *114*, 4429.

(24) Tanigaki, K.; Ebbesen, T.-W.; Kuroshima, S. *Chem. Phys. Lett*. **1991**, *185*, 189.

(25) Rentzepis, P. M. *Chem. Phys. Lett*. **1968**, *2*, 117; **1967**, *3*, 717.

(26) Murata, S.; Inagawa, C.; Toda, T.; Kokobun, H. *Chem. Phys. Lett*. **1972**, *13*, 101; **1973**, *15*, 152.

(27) Geldof, R. A.; Rettschnick, R. P. H.; Hoytink, G. J. *Chem. Phys. Lett*. **1969**, *4*, 59.

(28) Wannier, P.; Rentzepis, P. M.; Jortner, J. *Chem. Phys. Lett.* **1971**, *10*, 102, 193.

(29) Deinum, T.; Werkhoven, C. J.; Langelaar, J.; Rettschnick, R. P. H.; van Voorst, J. D. W. *Chem. Phys. Lett*. **1973**, *19*, 29.